Available online at www.sciencedirect.com
SCIENCE DIRECT®
Journal of Solid State Chemistry 177 (2004) 1292–1296
JOURNAL OF SOLID STATE CHEMISTRY
http://elsevier.com/locate/jssc

Synthesis and photoluminescence of the $Y_2O_3:Eu^{3+}$ phosphor nanowires in AAO template

Jilin Zhang and Guangyan Hong*

Key Laboratory of Rare Earth Chemistry and Physics, Changchun Institute of Applied Chemistry, Chinese Academy of Sciences, Changchun 130022, People's Republic of China

Received 16 June 2003; received in revised form 1 November 2003; accepted 6 November 2003

Abstract

The monodisperse array and nanowires of $Y_2O_3:Eu^{3+}$ phosphor were synthesized using anodic aluminum oxide (AAO) template by sol–gel method. Scanning electron microscope (SEM) images indicated that $Y_2O_3:Eu^{3+}$ nanowires are parallelly arranged, all of which are in uniform diameter of about 50 nm. The high-magnification SEM image showed that each nanowire is composed of a lot of agglutinating particles. The patterns of selected-area electron diffraction confirmed that $Y_2O_3:Eu^{3+}$ nanowires mainly consist of polycrystalline materials. Excitation and emission spectra of $Y_2O_3:Eu^{3+}$/AAO composite films were measured. The characteristic red emission peak of Eu^{3+} ion attributed to $^5D_0 \rightarrow {}^7F_2$ transition in $Y_2O_3:Eu^{3+}$/AAO nanowires broadened its halfwidth.

Keywords: Nanowires; $Y_2O_3:Eu^{3+}$; AAO template; luminescence

1. Introduction

In recent years, nanocrystalline $Y_2O_3:Eu^{3+}$ phosphor has received considerable interest in both fundamental and applied studies, for instance, in the characteristics of the spectra and field emission display, etc., due to its excellent luminescence efficiency, color purity, and stability [1]. In the preparation of nanocrystalline $Y_2O_3:Eu^{3+}$ phosphor, many different techniques such as spray pyrolysis [2], chemical vapor deposition [3], sol–gel [4] and so on have been reported. But it is difficult for these methods to obtain narrow particles size distribution and prevent the aggregation of particles.

The sol–gel synthesis in anodic aluminum oxide (AAO) template has been widely used for the preparation of semiconductor oxides (such as TiO_2, MnO_2, Co_3O_4, ZnO, WO_3, and SiO_2, etc.), composite nanostructure materials and nanowires [5]. This method for synthesis of inorganic materials has a number of advantages over conventional synthetic procedures. For example, monodisperse arrays of nanoparticles with uniform diameters can be synthesized. Moreover, this can effectively prevent the aggregation of particles because the nanoparticles are isolating each other. In addition, the tubules and fibrils of the desired material can be obtained after the AAO template is removed by chemical etching. But the AAO templates used by sol–gel template synthesis are almost unsupported AAO films with penetrated pores. During the preparation of AAO unsupported films need stripping off the remaining Al metal layer and opening the bottom caps of AAO by means of chemical etching; this is time-consuming [6–7]. Recently, Gaponenko [8] reported the Er- and Tb-doped SiO_2, TiO_2, Fe_2O_3, Al_2O_3, In_2O_3 luminescent films in porous anodic alumina on a silicon substrate using sol–gel method by spin-on or dip coatings. However, to our knowledge, monodisperse array and nanowires of $Y_2O_3:Eu^{3+}$ synthesized by AAO template have not yet been thoroughly investigated [9–10].

In this work, we made an attempt to synthesize monodisperse array and nanowires of $Y_2O_3:Eu^{3+}$ using a supported AAO template by sol–gel method. The experimental results demonstrated that the method can be applied to assemble $Y_2O_3:Eu^{3+}$ nanostructure materials. At the same time, the broadening of Eu^{3+} emission peak at around 611 nm was observed.

*Corresponding author. Fax: +86-431-5698-041.
E-mail address: gyhong@ns.ciac.jl.cn (G. Hong).

0022-4596/$ - see front matter © 2003 Elsevier Inc. All rights reserved.
doi:10.1016/j.jssc.2003.11.013

2. Experimental

Nanoporous AAO templates were prepared by a two-step anodizing process [11,12]. After high-purity aluminum plate (99.999%, 11 cm × 4 cm × 0.5 mm) was annealed at 500°C for 3–5 h in air and degreased in acetone, one side of the aluminum plate (as anode) under the protection of both Teflon plates with 20 cm^2 window in one of this was electropolished to a mirror finish in a 1:5 (v/v) perchloric acid/ethanol solution at 5–15°C for 3 min at a current density of 450 mA/cm^2. The polished anode was oxidized at a constant potential (40 V) in 0.3 M oxalic acid ($C_2H_2O_4$) at 1–3°C for 10 h. The anode was then immersed in an aqueous solution of 0.6 M H_3PO_4 and 0.15 M H_2CrO_4 at 60°C for 48 h to remove the alumina layer. Subsequently, the anode was anodized for 10 h in the same condition again and became AAO template with highly ordered nanoporous arrays (namely supported AAO template).

Y_2O_3:Eu^{3+} sol was prepared as follows. Y_2O_3 (4 N, 0.5000 g) and Eu_2O_3 (4 N, 0.04674 g) were dissolved in 2.5 mL of 1:1 (v/v) HNO_3 by stirring the mixture at 80–90°C. The solution was continuously heated to remove the excess H_2O and HNO_3, and then slightly cooled down. After this solution was added into 150 mL of deionized water and adjusted pH to 4–5 with 1:9 (v/v) $NH_3 \cdot H_2O$, the solution was concentrated by slow evaporation at 60–70°C with stirring and finally turned into a transparent Y_2O_3:Eu^{3+} hydrosol.

The AAO was dipped into Y_2O_3:Eu^{3+} hydrosol for 20–30 min, removed, and allowed to dry in air for 2 h. The template was then placed in a tube furnace (in air), and the temperature was ramped (2.5°C/min) to 800°C. The template was heated at this temperature for 2 h, and the temperature was ramped back down (2.5°C/min) to room temperature. Subsequently, we polished the template surface with abrasive paper so as to clean out the adhesive substances. Finally, we got the sample of Y_2O_3:Eu^{3+}/AAO. The sample was then cut into three sections marked S1, S2 and S3, respectively. The S2 and S3 samples were heated at 900°C and 1000°C, respectively, for 2 h in air. The speed of temperature increasing or decreasing was 2.5°C/min.

The morphologies of the AAO template and the Y_2O_3:Eu^{3+}/AAO nanowires were characterized by a PHILIPS XL30 ESEM FEG scanning electron microscope (SEM). The energy dispersive X-ray (EDX) spectrum of the Y_2O_3:Eu^{3+}/AAO sample was obtained using this instrument. The morphology and the selected-area electron diffraction (SAED) pattern of a single Y_2O_3:Eu^{3+}/AAO nanowire were determined by a JEOL JEM-2010 transmission electron microscope (TEM). The XRD pattern of the sample was examined by a Rigaku Dmax-B X-ray diffractometer. PL spectra of the sample were measured by a HITACHI F-4500 FL spectrophotometer equipped with a 150-W xenon lamp as the excitation source at room temperature.

Before the SEM observation, the Y_2O_3:Eu^{3+}/AAO sample was etched by 6 M aqueous NaOH for 1 h. This sample was attached to a sample stub with adhesive tape and sputtered with a thin layer of Au onto the surface. For the TEM observation, a piece of the resulting sample was placed onto a carbon-film-coated TEM grid. The 6 M aqueous NaOH solution was then applied to the sample in order to dissolve the alumina and substrate Al.

3. Results and discussion

3.1. Morphologies and structure

Fig. 1 presents the SEM image of a supported AAO template. The image demonstrates that the AAO template has highly ordered nanoporous arrays with diameters of approximately 50 nm. Fig. 1a is a larger area image of a supported AAO template and Fig. 1b is a magnification image of the selected-area image in Fig. 1a.

SEM and EDX observations of the Y_2O_3:Eu^{3+} nanowires (Fig. 2) show that the Y_2O_3:Eu^{3+} is filled

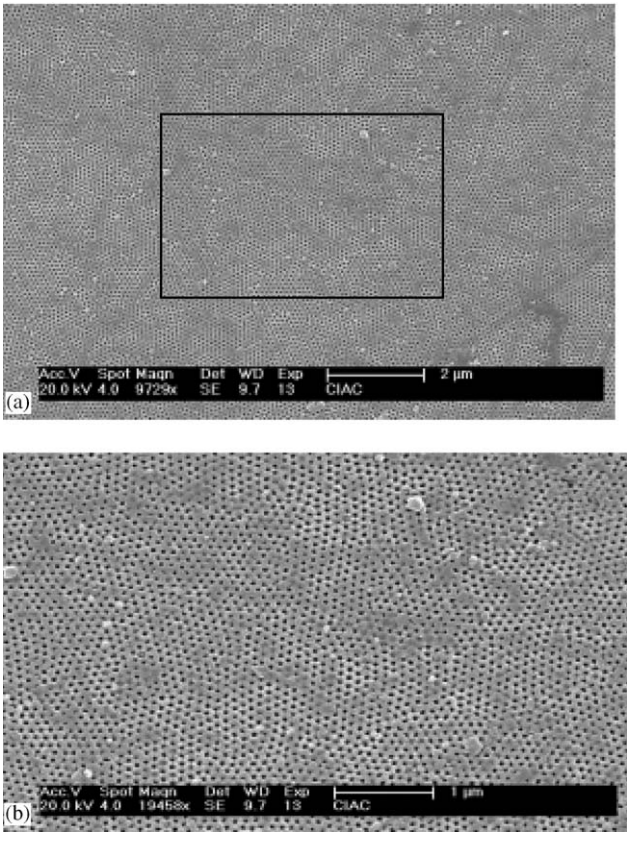

Fig. 1. SEM images of a supported AAO template.

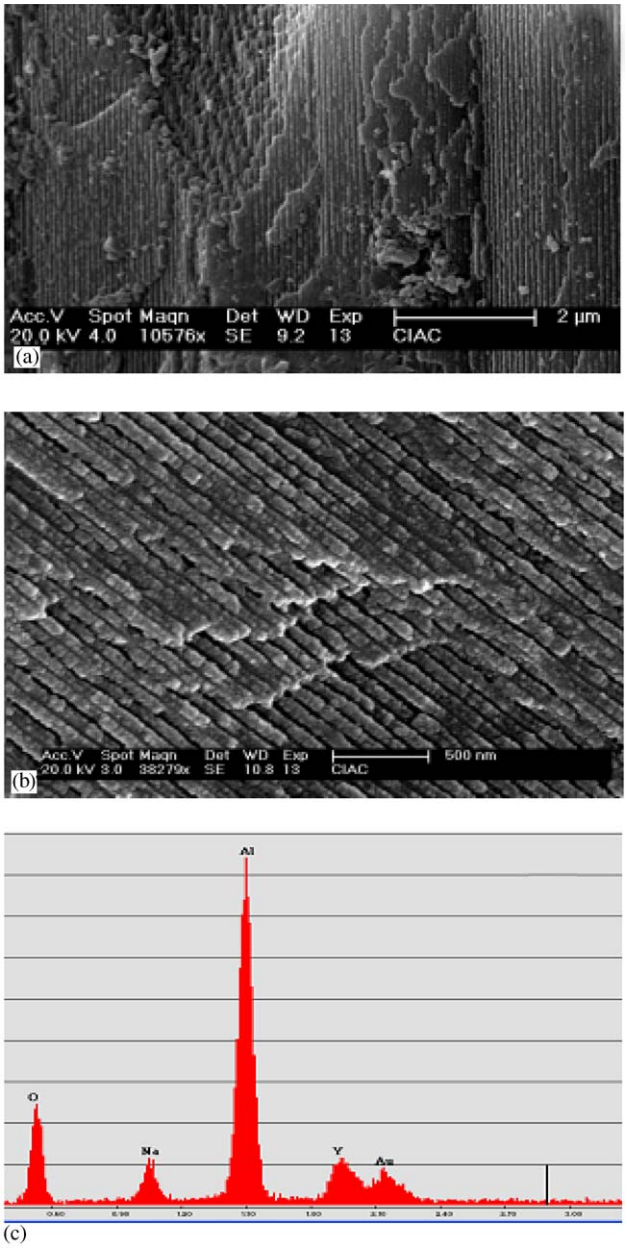

Fig. 2. SEM images (a and b), and EDX analysis spectrum (c) of the nanowires of Y_2O_3:Eu^{3+}.

into the AAO template and formed nanowires. It can be clearly seen that the Y_2O_3:Eu^{3+} are parallelly arranged, all of which are in a uniform diameter of about 50 nm. The diameter of these nanowires matches well with the pore diameter of the AAO template. The high-magnification SEM image indicates that each nanowire is composed of many agglutinating particles. The EDX spectrum shows that the chemical composition of Y_2O_3:Eu^{3+}/AAO/Al composite is mostly Al, O, and Y; as expected, minor quantities of Na and Au are also present, while the quantities of Eu are too scarce to be detected. However, the following sensitive photoluminescence spectra data in Fig. 5 can confirm existence of Eu^{3+} in Y_2O_3:Eu^{3+} nanowires.

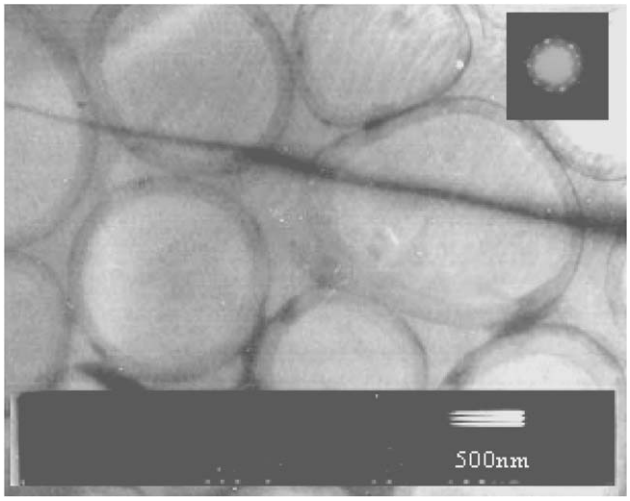

Fig. 3. TEM image of a single Y2O3:Eu^{3+} nanowire; inset, SAED pattern taken from the nanowire.

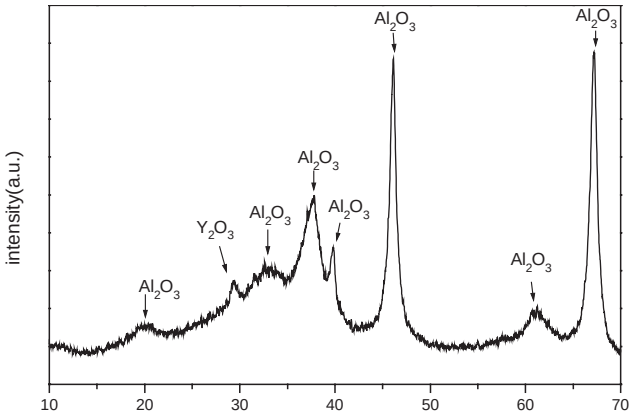

Fig. 4. XRD pattern of the Y_2O_3:Eu^{3+}/AAO/Al composite film.

A single nanowire with a diameter of about 50 nm is observed by the TEM image in Fig. 3. The SAED pattern (Fig. 3, inset), taken from the single nanowire shown in Fig. 3, reveals some diffraction spots and diffusive rings. This means that the nanowire of Y_2O_3:Eu^{3+} may be composed of polycrystalline and amorphous materials. Further evidence comes from the X-ray diffraction of the Y_2O_3:Eu^{3+}/AAO/Al composite film in Fig. 4. The XRD result indicates that the diffraction peaks are assigned to Y_2O_3 and γ-Al_2O_3 of AAO template without metal Al. We can merely observe one widening diffraction peak of Y_2O_3 at around $2\theta = 29.235^\circ$ corresponding to cubic (222) plane. The reason for weaker diffraction peaks of Y_2O_3 could be due to a little quantity of Y_2O_3 in AAO template and the absence of adhesive Y_2O_3 on the surface of AAO template. The thicker AAO membrane on metal Al could be the reason why the diffraction peaks of metal

Al are too weak to be detected. While the widening of the diffraction peaks of Y_2O_3 may provide some evidence of smallness of the crystalline particles or being amorphous.

3.2. Photoluminescence spectra

Under the same conditions, the excitation and emission spectra of S1, S2, and S3 samples are shown in Fig. 5. From this characteristic spectra we can further confirm that the Y_2O_3:Eu^{3+}/AAO nanowires are mainly composed of cubic phase. In Fig. 5(a), the excitation spectra were measured by monitoring the emission wavelength at 611 nm. There are three sets of lines to be observed: one broad and strong band at about 254 nm is an $O^{2-} \rightarrow Eu^{3+}$ charge transfer transition from an oxygen 2p state excited to an Eu^{3+} 4f state, three narrow and weak bands at around 365, 381 and 396 nm consisting of one set of peaks; while another single peak is located at 466 nm, these peaks are derived from

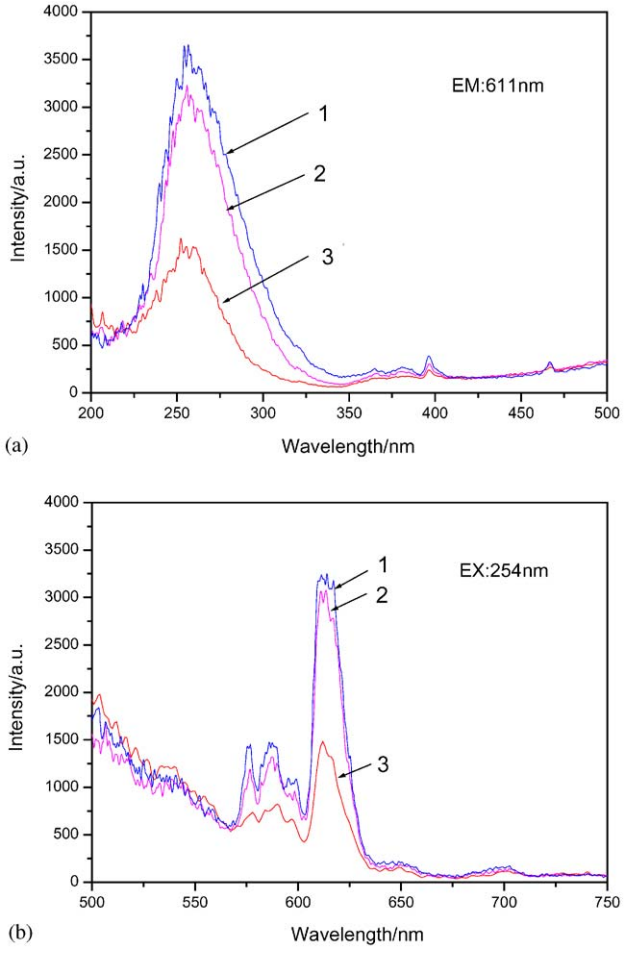

Fig. 5. PL spectra of the Y_2O_3:Eu^{3+}/AAO composite film: (a) excitation, and (b) emission spectra: 1—S1(1000°C), 2—S2(900°C), and 3—S3(800°C).

$^7F \rightarrow {}^5D$ absorbing transition of 4f electrons of Eu^{3+}. Under 254 nm UV light excitation, we have observed the characteristic red emission peak of Eu^{3+} ions in Fig. 5(b). The peak is due to the $^5D_0 \rightarrow {}^7F_2$ forced electric dipole transition of Eu^{3+}. However, we found that this emission peak of the Y_2O_3:Eu^{3+}/AAO in three different firing temperatures exhibited a broadened line width of about 17 nm halfwidth and the halfwidth almost did not change with the increase of firing temperature. This phenomenon that the spectral lines of Eu^{3+} at 611 nm of nanocrystalline Y_2O_3:Eu^{3+} phosphors are much broader than those of the bulk materials has also been presented and there is a generally accepted theory that the broadening in these spectra is attributed to inhomogeneous broadening caused by the surface and interface effects of the small particles [13–16]. Our preliminary experimental results also support the conclusion. The reasons are as follows. First, under the same conditions, the halfwidth of 611 nm emission peak of Eu^{3+} did not decrease with the increase of firing temperature. This shows amorphous materials were not the main reason for the spectral line broadening. Second, SEM results have confirmed Y_2O_3:Eu^{3+} nanowires are composed of many agglutinated nanoparticles. Thus structural defect and disorder crystal lattice of the Y_2O_3:Eu^{3+} nanowires exist everywhere.

4. Conclusions

The monodisperse array and nanowires of Y_2O_3:Eu^{3+} phosphor with uniform particle size were synthesized using AAO template by sol–gel method. The Y_2O_3:Eu^{3+} nanowires are parallelly arranged in AAO template, all of which have uniform diameter of about 50 nm and are mainly composed of polycrystalline particles with cubic phase. The red emission peak of Y_2O_3:Eu^{3+}/AAO at 611–616 nm is attributed to $^5D_0 \rightarrow {}^7F_2$ forced electric dipole transition of Eu^{3+}; this emission peak exhibited a broadened line width.

Acknowledgments

This work was financially supported by the National Science Foundation of China (Grant No. 20071031).

References

[1] G. Wakefield, E. Holland, P.J. Dobson, J.L. Hutchison, Adv. Mater. 13 (2001) 1557.
[2] Y.C. Kang, H.S. Roh, S.B. Park, J. Electrochem. Soc. 147 (2000) 1601.
[3] L.D. Sun, J. Yao, C. Liu, C. Liao, C.H. Yan, J. Lumin. 87–89 (2000) 447.

[4] M.H. Lee, S.G. Oh, S.C. Yi, J. Colloid Interface Sci. 226 (2000) 65.
[5] B.B. Lakshmi, C.J. Patrissi, C.R. Martin, Chem. Mater 9 (1997) 2544.
[6] Yingke Zhou, Chengmin Shen, Hulin Li, Solid State Ionics 146 (2002) 81.
[7] G. Shi, C.M. Mo, W.L. Cai, L.D. Zhang, Solid State Commun. 115 (2000) 253.
[8] N.V. Gaponenko, Synth. Met. 124 (2001) 125.
[9] R. Schmechel, M. Kennedy, H. von Seggern, H. Winkler, M. Kolbe, R.A. Fischer, Li Xaomao, A. Benker, M. Winterer, H. Hahn, J. Appl. Phys. 89 (2001) 1679.
[10] R. Schmechel, H. Winkler, Li. Xaomao, M. Kennedy, M. Kolbe, A. Benker, M. Winterer, R.A. Fischer, H. Hahn, H. von Seggern, Scr. Mater. 44 (2001) 1213.
[11] A.P. Li, F. Müller, A. Birner, K. Nielsch, U. Gösele, J. Appl. Phys. 84 (1998) 6023.
[12] Y.C. Sui, J.M. Saniger, Mater. Lett. 48 (2001) 127.
[13] H.S. Peng, H.W. Song, B.J. Chen, S.Z. Lu, S.H. Huang, Chem. Phys. Lett. 370 (2003) 485.
[14] D.K. Williams, B. Bihari, B.M. Tissue, J. Appl. Phys. 102 (1998) 916.
[15] W.P. Zhang, Y. Min, Chin. J. Lumin. 12 (2001) 314.
[16] S.Z. Lu, D. Li, S.H. Huang, Acta Opt. Sinica 21 (2001) 1084.